MOLECULAR PAIN

Original Article

Molecular Pain
Volume 12: 1–17

DOI: 10.1177/1744806916628734
mpx.sagepub.com
SAGE

Functional and structural characterization of axonal opioid receptors as targets for analgesia

Egle M Mambretti, PhD student[1,2], Katrin Kistner, PhD[3], Stefanie Mayer, MS[4], Dominique Massotte, PhD[5], Brigitte L Kieffer, PhD[6,7], Carsten Hoffmann, PhD[4], Peter W Reeh, MD[3], Alexander Brack, MD[1], Esther Asan, MD[2] and Heike L Rittner, MD[1]

Abstract

Background: Opioids are the gold standard for the treatment of acute pain despite serious side effects in the central and enteric nervous system. μ-opioid receptors (MOPs) are expressed and functional at the terminals of sensory axons, when activated by exogenous or endogenous ligands. However, the presence and function of MOP along nociceptive axons remains controversial particularly in naïve animals. Here, we characterized axonal MOPs by immunofluorescence, ultrastructural, and functional analyses. Furthermore, we evaluated hypertonic saline as a possible enhancer of opioid receptor function.

Results: Comparative immunolabeling showed that, among several tested antibodies, which all provided specific MOP detection in the rat central nervous system (CNS), only one monoclonal MOP-antibody yielded specificity and reproducibility for MOP detection in the rat peripheral nervous system including the sciatic nerve. Double immunolabeling documented that MOP immunoreactivity was confined to calcitonin gene-related peptide (CGRP) positive fibers and fiber bundles. Almost identical labeling and double labeling patterns were found using mcherry-immunolabeling on sciatic nerves of mice producing a MOP-mcherry fusion protein (MOP-mcherry knock-in mice). Preembedding immunogold electron microscopy on MOP-mcherry knock-in sciatic nerves indicated presence of MOP in cytoplasm and at membranes of unmyelinated axons. Application of [D-Ala^2, N-MePhe^4, Gly-ol]-enkephalin (DAMGO) or fentanyl dose-dependently inhibited depolarization-induced CGRP release from rat sciatic nerve axons ex vivo, which was blocked by naloxone. When the lipophilic opioid fentanyl was applied perisciatically in naïve Wistar rats, mechanical nociceptive thresholds increased. Subthreshold doses of fentanyl or the hydrophilic opioid DAMGO were only effective if injected together with hypertonic saline. In vitro, using β-arrestin-2/MOP double-transfected human embryonic kidney cells, DAMGO as well as fentanyl lead to a recruitment of β-arrestin-2 to the membrane followed by a β-arrestin-2 reappearance in the cytosol and MOP internalization. Pretreatment with hypertonic saline prevented MOP internalization.

Conclusion: MOPs are present and functional in the axonal membrane from naïve animals. Hypertonic saline acutely decreases ligand-induced internalization of MOP and thereby might improve MOP function. Further studies should explore potential clinical applications of opioids together with enhancers for regional analgesia.

Keywords

μ-Opioid receptor, internalization, peripheral nerve, ultrastructure, hypertonic solution, DAMGO, fentanyl, calcitonin gene-related peptide

Date received: 30 July 2015; accepted: 10 October 2015

[1]Department of Anesthesiology, University Hospital of Wuerzburg, Germany
[2]Institute of Anatomy and Cell Biology, University of Wuerzburg, Germany
[3]Institute of Physiology and Pathophysiology, University of Erlangen-Nuremberg, Germany
[4]Institute for Pharmacology and Toxicology & Bio-Imaging Center/Rudolf-Virchow Center, University of Wuerzburg, Germany
[5]Institut des Neurosciences Cellulaires et Intégratives, CNRS UPR, Strasbourg Cedex, France
[6]Douglas Research Center, Department of Psychiatry, Faculty of Medicine, McGill University, Montreal, Quebec, Canada
[7]Institut de Génétique et de Biologie Moléculaire et Cellulaire, Université de Strasbourg, Illkirch, France

Corresponding author:
Heike L Rittner, Department of Anesthesiology, University Hospital of Wuerzburg, Oberdürrbacher Straße 6, D-97080 Würzburg, Germany.
Email: rittner_h@ukw.de

Background

μ-Opioid receptors (MOPs) are expressed both in the central and peripheral nervous system where they play a pivotal role in analgesia. However, systemic application for pain treatment has several side effects, like nausea and respiratory depression as well as tolerance and addiction.[1] In fact, in closed claim studies on anesthesia-related morbidity and mortality, opioid-induced respiratory depression is the most important reason for death or severe brain damage.[2] To avoid systemic side effects, peripheral administration of opioids to selectively target MOP in nociceptors is an alternative.

Peripheral opioid receptors are transcribed in perikarya of sensory neurons in the dorsal root ganglion (DRG) and are transported along the axons to their terminals.[3,4] While opioid receptor expression[5] and function has been conclusively demonstrated at nerve terminals,[6–8] it remains controversial whether they are expressed in the membrane of peripheral nociceptive axons and whether opioid receptor agonists can induce antinociception when applied at the axon. Under pathologic conditions, e.g. in animals with neuropathy caused by nerve injury, exogenous as well as endogenous MOP agonists applied at the damaged nerve can elicit potent antinociception or anti-allodynia.[9–12] In contrast, in naïve animals, no antinociception to thermal nociceptive stimuli was seen in rats after application of fentanyl and morphine alone.[13] In clinical settings, hydrophilic and hydrophobic opioids like morphine, fentanyl, alfentanil, buprenorphine, and butorphanol have been used not as sole analgesics but as adjuvants to local anesthetics in regional anesthesia via application in nerve blocks[14] or via intravenous regional anesthesia using a tourniquet approach.[15] To date, there are still conflicting results whether the addition of opioids to local anesthetics improves regional anesthesia. No larger clinical studies have been conducted using opioids alone.

An apparent failure of perineurally injected opioids to exert antinociception in intact nerves could be caused either by a lack of functional opioid receptors in the axonal membranes under physiological conditions, or by the inability of injected opioids to cross the intact perineurial barrier and to reach nociceptors. Indeed, application of the hydrophilic opioid [D-Ala^2, N-MePhe^4, Gly-ol]-enkephalin (DAMGO) at the sciatic nerve in naïve rats elicits mechanical antinociception when it is accompanied by treatments suited to open the perineurial barrier, such as coinjection of hypertonic saline.[16–18] This finding indicates that, under these conditions, axonal MOPs are available and functional. However, it remains to be determined (1) whether hypertonic saline-mediated barrier breakdown alone is sufficient to allow opioid-induced antinociception on MOPs constitutively present in axonal membranes of nociceptors or (2) whether hypertonic saline treatment exerts additional influence directly on MOP availability and function similar to its effects in non-inflamed peripheral tissue.[19]

MOP activates several signaling cascades including G(i)-protein-dependent and -independent signaling pathways,[20] e.g. activation of adenylate cyclase, phosphorylation by protein kinases, activation of specific potassium[21] and calcium channels,[22] and β-arrestin recruitment. Following ligand binding, MOP is desensitized, e.g. by phosphorylation indicating an acute loss of MOP-effector coupling within seconds to minutes. Desensitization can be followed by internalization of MOP via β-arrestin as a scaffolding molecule.[23] After internalization of MOP, the receptor can be reinserted as a non-desensitized/reactivated receptor in the plasma membrane. MOP internalization induced by the agonists enkephalin or etorphine can be blocked by hypertonic sucrose.[24] Whether this applies to hypertonic saline solutions as well is currently unknown.

To address all of these questions, this study was designed to analyze the presence and function of MOPs in nociceptive axons under physiological conditions. Since previous studies had shown very low levels of MOP in intact peripheral nerves,[3] and significant unspecific labeling of polyclonal MOP-antibodies in peripheral nervous tissue,[3] we tested various commercially available antibodies to achieve optimal MOP detection in rat sciatic nerve. Additionally, we took advantage of a previously characterized genetic mouse model with a knocked-in fluorescent protein tag into the *Oprm1* of MOP[25] to perform comparative light and ultrastructural MOP localization studies with a higher specificity and signal-to-noise ratio than achievable using an antibody against the wild-type (WT) MOP sequence.

Functionality of MOPs in sensory axons was assessed by studying MOP agonist-triggered inhibition of CGRP release from isolated sciatic nerve preparations and in vivo in rats by performing pain behavioral tests after perisciatic application of the lipophilic opioid fentanyl without coinjection treatment. Furthermore, the effect of hypertonicity on opioid-induced antinociception in vivo or on β-arrestin-2 recruitment and MOP internalization was evaluated in vitro in MOP – β-arrestin-2 double-transfected cells.

Material and Methods

Rats, MOP-mcherry knock-in mice

Animal experiments were performed in accordance with the European Communities Council Directive of 26 May 2010 and approved by the local animal care committees (Regierung von Unterfranken, Wuerzburg, Germany and Regierung von Mittelfranken, Ansbach, Germany, Com'Eth 2010-003 Strasbourg, France). They were

conducted in accordance with the International Association for the Study of Pain.[26] At the end of the experiment, animals were sacrificed using an intracardial injection of a solution of T61 (embutramide, mebezonium, and tetracaine) or intracardial perfusion with 4% paraformaldehyde (PFA) both under isoflurane anesthesia according to national guidelines (see below). Animals were kept at 22°C with a light-dark circle of 12 h. Animals had access to food and water ad libitum.

Wistar male rats (Janvier, Saint-Berthevin Cedex, France), weighing 180–200 g, were used for imaging, behavior, and CGRP release experiments as described below.

Male and female homozygous knock-in mice aged six to 12 weeks were used. MOP-mcherry knock-in mice were generated by homologous recombination.[25] The mcherry cDNA was introduced into exon 4 of the MOP gene, in frame and 5′ of the stop codon. This C-terminal construct was designed to allow correct native-like MOP expression at subcellular level to visualize the MOP protein expressing neuronal population. The genetic background of all mice was C57/BL6J;129svPas (50:50%). Functional properties of MOP are maintained in MOP-mcherry mice both in vitro and in vivo.[25]

Genotyping

Mice genotyping was performed by standard PCR technique using a 5′ oligonucleotide located on the fourth exon of the oprm1 gene (BAZ 43 tgacgtgacatgcagttgagattt, Eurofins) and a 3′ oligonucleotide located in the 3′ untranslated region (BAZ 44 tcccacaaaccctgacagcaac, Eurofins). Introduction of the coding sequence for mcherry increased the size of the amplified fragment by about 800 bp enabling identification of WT oprm1 -/-, heterozygous oprm1 -/mch, and homozygous oprm1 mch/mch (MOP-mcherry knock-in) animals by PCR. Ear samples were analyzed as described before.[25]

Immunofluorescence

Rats and mice were perfused under deep isoflurane anesthesia via the left ventricle. A brief prerinse with heparinized saline was followed by fixation (4% PFA in 0.1 M phosphate buffer (pH 7.4)) and a postfixation over night at 4°C. Subsequently, tissues were dissected, cryoprotected with 10% and 20% sucrose in 0.01 M phosphate-buffered saline (PBS), embedded in O.C.T. (O.C.T. Compound, code 4583, Tissue-Tek, Sakura), frozen in liquid nitrogen-cooled 2-methylbutane, and stored at −80°C until use. Frozen tissue was sectioned in 10 µm cryosections (cryostat CM 3050 S, Leica) and collected on glass slides (Superfrost™ Plus Microscope Slides, code J1800AMNZ, Thermo Scientific) or cut at 30 µm and collected in a 24-well plate in PBS (free-floating section). Free-floating sections were used immediately after cutting; cryostat sections on glass slides were immediately used or stored at −80°C.

Immunostaining was performed on brain, spinal cord, DRG, and sciatic nerve. Cryostat sections from rat tissue were washed in PBS followed by blocking in PBS/0.5% Triton-X-100/5% normal goat serum for 2 h. Subsequently, primary antibody incubation was carried out overnight at 4°C in PBS/0.5% Triton X-100/1% normal goat serum using the appropriate concentration of one or, for dual labeling, two antibodies from different species (rabbit-anti-MOP (MOP_1), polyclonal, #ab10275, 1:500–1:800, Abcam, Cambridge, UK; rabbit-anti-MOP (MOP_2), polyclonal, #RA10104, 1:600–1:800, Neuromics, Edina, MN, USA; guinea pig-anti-MOP, polyclonal, #ab64746, Abcam; guinea pig-anti-MOP, polyclonal, #GP10106, Neuromics; rabbit-anti-MOP, monoclonal, #ab134054, 1:250–500, (RabMAb-MOP), Abcam; mouse-anti-CGRP, monoclonal, #ab81887, 1:400, Abcam). Free-floating sections were kept in slight movement. Then, samples were washed in PBS and incubated for 2 h at room temperature with appropriate secondary antibody or combination of antibodies (Cy3-labeled anti-rabbit, 1:400–800, Cy2-labeled anti-mouse, 1:400; Jackson Immuno Research, West Grove, PA, USA), treated for nuclear counterstain with 4′,6-diamidino-2-phenylindole (DAPI) and mounted with mounting medium (Fluorogel, #17985–11, Electron Microscopy Sciences). Controls (omission of one or both primary antibodies) were carried along for each immunolabeling experiment. In dual labeling, cross reactivity controls treated with only one of the two primary antibodies but both secondary antibodies were also performed. All controls lacked specific staining.

Immunofluorescence on mouse tissue was carried out on cryosections as described,[25] with overnight incubation at 4°C using rabbit-anti-mcherry antibody (DsRed; #632496, 1:1000, Clontech, Mountain View, CA, USA) alone or in combination with anti-CGRP (see above). Free-floating sections were kept in slight movement. No specific labeling was found after omission of primary antibodies in all tissue samples from WT and homozygous MOP-mcherry knock-in mice. Labeling was also absent in brain sections of WT mice incubated with the anti-mcherry antibody. Observation and image acquisition was done with the BZ-9000 BIOREVO (Keyence) or an Olympus BHS epifluorescence microscope equipped with the appropriate filter systems.

Electron microscopy

Preembedding immunogold labeling of sciatic nerve. After perfusion, overnight postfixation, and washing steps as

described above, sciatic nerve from rat, MOP-mcherry knock-in and WT mice were coronally cut into small pieces (~3 mm). Immunolabeling was carried out with RabMAb-MOP for rat and anti-mcherry antibody for mouse preparations and detected using ultrasmall gold-conjugated secondary antibodies (goat-anti-rabbit US, #100.011, 1:50, Aurion, Wageningen, Netherlands) and silver-enhancement according to Bonn et al.[27] Control incubations included omission of primary antibody and incubation of WT mouse sciatic nerve with and without mcherry antibody. After labeling, preparations were osmicated, dehydrated in ethanol, and embedded in Epon.[27] Serial coronal ultrathin sections (70 nm) were cut at 5 µm from the surface, collected onto 500 mesh formvar-coated nickel grids, contrasted with uranyl acetate and lead citrate,[28] and observed with the transmission electron microscope LEO AB 912 (Zeiss NTS, Oberkochen, Germany). Micrographs of Remak bundles and myelinated axons were taken at 6300 × magnification using a CCD camera (Sharp:eye CCD camera controller und TEM-camera, TRS Tröndle, Germany).

Analysis of immunogold labeling. Individual Remak bundles and myelinated axons in their vicinity were identified in micrographs of serial ultrathin sections of the following preparations: MOP-mcherry knock-in mouse sciatic nerve reacted with/without mcherry antibody (MOP-mcherry pos/neg); WT mouse sciatic nerve reacted with/without mcherry antibody (WT-pos/neg). For each identified Remak bundle, micrographs of three to five serial sections were analyzed. The number of silver-intensified immunogold dots (IG) and the Remak bundle area (determined using Image J 1.49 t, NIH, USA), comprising unmyelinated axons and the surrounding Schwann cell cytoplasm, excluding the Schwann cell nucleus, were determined. By directly comparing micrographs of serial sections, it was ensured that gold dots were not counted twice. Dot density was calculated as n°dots (DR)/area (AR) for each individual Remak bundle. Since most of the myelinated fibers surrounding the Remak bundles were thickly myelinated, presumably MOP-negative fibers, overall dot density over myelinated fibers (including axon, myelin sheath, and Schwann cell cytoplasm, excluding Schwann cell nucleus) was determined as intrasectional background labeling. Thereafter, a labeling enrichment for each Remak bundle was calculated by dividing its individual dot density value by the background density value determined in the same micrographs, and a mean labeling enrichment was calculated for the Remak bundles analyzed in each preparation (between 10 and 15).

Western blotting

Rat and mouse tissues were homogenized in radioimmunoprecipitation assay (RIPA) buffer (25 mM HEPES pH 7.6, 2 mM EDTA, 25 mM NaF, 1% (v/v) SDS) containing protease inhibitors (Complete; Roche Applied Science, Mannheim, Germany) and centrifuged at 10,000 r/min for 10 min at 4°C.[17,29] Protein concentration in the supernatant was determined using bicinchoninic acid (BCA) protein assay (Thermo Scientific, Rockford, IL, USA, Pierce BCA Protein Assay Kit). Fifty (brain and spinal cord) or 100 µg (DRG and sciatic nerve) protein in RIPA w/o complete and Laemmli buffer were denatured at 95°C for 5 min, fractionated on sodium dodecyl sulfate polyacrylamide gels, and subsequently blotted on nitrocellulose membranes (GE Healthcare UK, Buckinghamshire, UK). Proteins were detected using the specific antibodies against MOP and mcherry (see above). As protein loading control β-actin (Sigma-Aldrich) was used. Chemiluminescence signal detection of bands was acquired with an Imager (Alpha Innotech, Santa Clara, CA, USA; FluorChem FC2 Imaging systems, Multilmage II).

CGRP release

Sciatic nerves from Wistar rats, sacrificed in an atmosphere of increasing CO_2 concentration, were prepared as described before including removal of the nerve sheaths (epi-perineurium).[17] Nerves were loosely wrapped around acrylic glass rods[30] and placed in synthetic interstitial fluid (SIF[31]) containing (in mM) NaCl 108, KCl 3.48, $MgSO_4$ 3.5, $NaHCO_3$ 26, NaH_2PO_4 1.7, $CaCl_2$ 1.5, sodium gluconate 9.6, glucose 5.5, and sucrose 7.6 continuously gassed with carbogen (95% O_2, 5% CO_2) to pH 7.4. All experiments were performed in a shaking bath at constant 37°C and according to a specific application scheme. This involved several incubation steps in test tubes containing SIF or test solutions lasting for 5 min each. After a washout period of 30 min, nerves were incubated as a first step in SIF to determine basal CGRP release. One group of preparations in the second step was preincubated with opioids alone or together with the MOP antagonist naloxone. Chemical stimulation with 60 mM potassium chloride in the presence of opioids and +/− naloxone occurred either in the third or fourth incubation step. This was followed by two incubations or one, respectively, in SIF to assess reversibility of stimulated CGRP release. The CGRP content of each obtained fluid sample was determined using a commercial enzyme immunoassay kit (Bertin Pharma, Montingy le Bretonneux, France). The EIA plates were measured photometrically using a microplate reader (Dynatech, Channel Islands, UK).

Measurement of mechanical nociceptive thresholds

In male Wistar rats, the right sciatic nerve was located using a 22-gauge needle connected to a nerve stimulator (Stimuplex Dig RC; Braun) under brief isoflurane anesthesia as previously described.[17] DAMGO, and naloxone hydrochloride dehydrate (#N7758 and #E7384, Sigma-Aldrich, St. Louis, MO, USA), as well as fentanyl (Janssen Cilac, Neuss, Germany) were injected perineurially as described in detail before.[17,32] In selected experiments, 300 μl of 10% NaCl was injected before fentanyl injection. The doses of fentanyl and DAMGO applied perineurially have been previously shown not to elicit systemic effects.[33]

Mechanical nociceptive thresholds of rats were determined before and 10 min after opioid injection (with or without 10% NaCl) using the paw pressure algesiometer (modified Randall-Sellito test; Ugo Basile, Comerio, Italy).[34] Pressure was applied using a blunt piston onto the dorsal surface of the hindpaw. The paw pressure threshold (weight, g) was defined as the pressure required eliciting paw withdrawal. The average of three measurements was calculated. Treatments were randomized and blinded.

β-Arrestin, MOP constructs, and cell culture

We used bovine β-arrestin-2 fused C-terminally to YFP, GRK2[35] as well as human MOP-CFP[23] for a triple transfection as described previously. HEK-293 cells were maintained in Dulbecco's modified Eagle medium with 4.5 g/l glucose, 10% fetal calf serum, 100 U/ml penicillin G, and 100 µg/ml streptomycin sulfate at 37°C, 7% CO_2.

Individual 24-mm glass coverslips were placed in six-well plates and coated for 20 min using 300 μl of poly-D-lysine (1 mg/ml). Poly-D-lysine was aspirated, and the glass coverslips were washed once with sterile PBS without Ca^{2+}. HEK-293 cells were seeded onto these coverslips resulting in approximately 40% confluence. The cells were transfected using Effectene according to the manufacturer's instructions with the following amounts of DNA for a six-well plate: 2.6 µg for hMOP-CFP, 0.5 µg for β-arrestin-2-YFP, and 1.0 µg for GRK2. All constructs were in pcDNA3. Medium was exchanged 24 h later, and cells were analyzed 48 h after transfection.

For measurements in the presence of dynasore (Sigma Chemical), cells were incubated with 80 µM dynasore (dissolved in 0.4% DMSO) for 30 min prior to ligand application at 37°C, 7% CO_2. For experiments with hypertonic saline, cells were incubated with 200 mM NaCl for 5 min at room temperature prior to measurements.

Confocal microscopy of cell cultures

All confocal microscopy experiments were performed on a Leica TCS SP8 scanning microscope (Leica, Wetzlar, Germany). Coverslips with transfected HEK-293 cells were mounted using an "Attofluor" holder (Molecular Probes, Eugene, Oregon, USA). Images were taken with a 63×1.40 Oil objective lens as described previously.[36] In brief, using the manufacturer's settings, CFP was excited with a 442-nm diode laser, and emission was detected from 450–505 nm using a Hybrid Detector. YFP was excited with the 514-nm line of the argon laser, and emission was detected with the Photomultiplier from 530–600 nm. Settings for recording images were kept constant: 512×512-pixel format, line average 4, frame average 2400 Hz. Merely, the gain and offset were adjusted for each measurement. Time series were recorded using the standard Leica software package (version 2.61). Pictures were taken at 15 s intervals for 10 min.

Quantification of β-arrestin-2-translocation was performed with the Leica Application Suite Advanced Fluorescence software package (LAS AF version 4.0.0.11706). Regions of interest (ROIs) were defined in the cytosol and quantified over the time recorded. Care was taken that slight movements of the cells did not result in misplacement of the defined ROIs either onto the membrane or into the nuclear region. To correct for possible photobleaching, control regions were defined that included whole cells and were used to correct the images in the cytosolic ROIs. To quantify β-arrestin-2-translocation, the resulting fluorescence intensity values were normalized to the initial value and plotted against time.

Statistical analysis

Statistical analysis was done using SigmaPlot 11.0, Systat Software Inc. In case of not normally distributed data, the test was performed on ranks. Data are displayed as mean ± SEM (pain behavior, CGRP release, β-arrestin recruitment) or median and percentiles (immunogold labeling analysis). If aliquots of one sample were exposed to different conditions or repeated measurements (RMs) from one animal were taken, one- or two-way RMs analysis of variance was used. Post hoc comparisons were performed by Bonferroni (behavior data), Scheffe post hoc test (CGRP release), or Dunn's test on ranks (immunogold quantification). Differences were considered significant if $p < 0.05$.

Results

Immunolabeling with antibody providing high specificity and reproducibility indicates MOP localization in intact rat peripheral nociceptive axons

Immunofluorescence labeling of rat brain sections using rabbit and guinea pig polyclonal antibodies resulted in

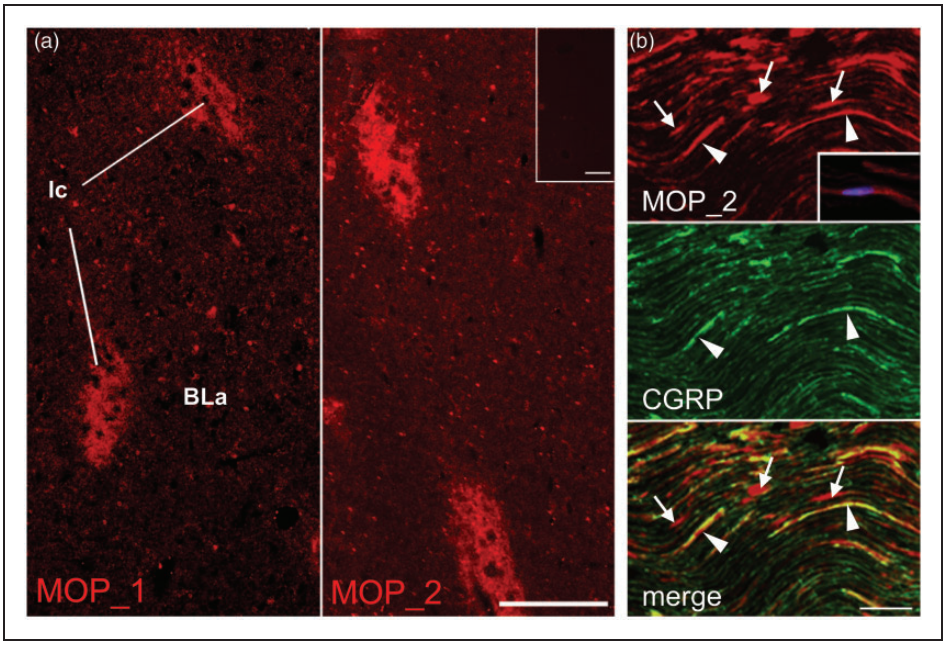

Figure 1. MOP-immunolabeling in rat amygdala and sciatic nerve using polyclonal antibodies. Rabbit polyclonal anti-MOP antibodies (MOP_1 and MOP_2) were used to label cryosections of brain and sciatic nerve. Specific MOP immunoreactivity was observed in (a) the paracapsular intercalated nuclei (Ic) of the amygdala. Inset shows lack of labeling in control section. Scale bars 100 μm. (b) In MOP_2-CGRP double-labeled longitudinal sections of sciatic nerves, CGRP-ir fibers/fiber bundles are labeled for MOP (arrowheads), but there are also numerous fluorescent signals outside CGRP-ir structures, which often, using DAPI couterstaining, are seen to contain nuclei and possess typical Schwann cell morphology (arrows and inset in upper image). Scale bar 50 μm.
BLa: basolateral amygdaloid nucleus; ir: immunoreactive; MOP: μ-opioid receptor; CGRP: calcitonin gene-related peptide; DAPI: 4′,6-diamidino-2-phenylindole.

consistently reproducible labeling patterns known from the literature on MOP localization in the CNS, e.g. in the paracapsular intercalated nuclei (Ic) of the amygdala.[37] Signal-to-noise ratio was higher for the rabbit (MOP_1, MOP_2; Figure 1(a)) than for the guinea pig antibodies (not shown). In the rat DRG, the different antibodies displayed varying and often inconsistent labeling patterns (not shown). Immunofluorescence labeling in the sciatic nerve was recognized in numerous fibers and fiber bundles, many of which were also positive for calcitonin gene-related peptide (CGRP), a marker for sensory axons. However, significant fluorescence signal was always present also in non-CGRP-immunoreactive (ir) structures, among them apparently numerous Schwann cells (Figure 1(b)). Control sections incubated without primary antibodies were devoid of fluorescence signal.

Immunofluorescence labeling using a monoclonal rabbit MOP-antibody (RabMAb-MOP) yielded specific and reproducible staining both in CNS areas (Ic, superficial laminae I/II of dorsal horn of spinal cord) and in small/medium DRG neurons (Figure 2(a)). In longitudinal sections of sciatic nerves (Figure 2(b)), MOP immunoreactivity was faint but clearly recognizable, often granular in appearance, and was localized to narrow fibers and fiber bundles. In phase contrast, these were situated between groups of large, myelinated non-reactive fibers (not shown). Dual labeling confirmed that CGRP was colocalized in all MOP-ir fibers and fiber bundles, providing evidence of MOP localization exclusively in sensory axons. Differential relative immunofluorescence intensities for MOP and CGRP in fibers and the presence of solely CGRP-ir fibers in double labeling both suggested preferential expression of MOP in subsets of sensory axons. No fluorescence signals were seen in non-CGRP-ir structures, e.g. Schwann cells, and control sections again were completely devoid of fluorescence signals. RabMAb-MOP detected a signal in Western blot at the predicted size in the rat brain and spinal cord (Figure 2(c)). Substantially less MOP protein was observed in the DRG and the sciatic nerve. In addition, other smaller and larger bands were seen in the peripheral nervous tissue, which could be due to post-translational modification.[38]

MOP-mcherry detection in MOP-mcherry knock-in mice validates localization of the fusion protein in mouse peripheral nociceptive axons

Mcherry fluorescence signal, enhanced with anti-mcherry (DsRed) antibody, was specifically localized in the

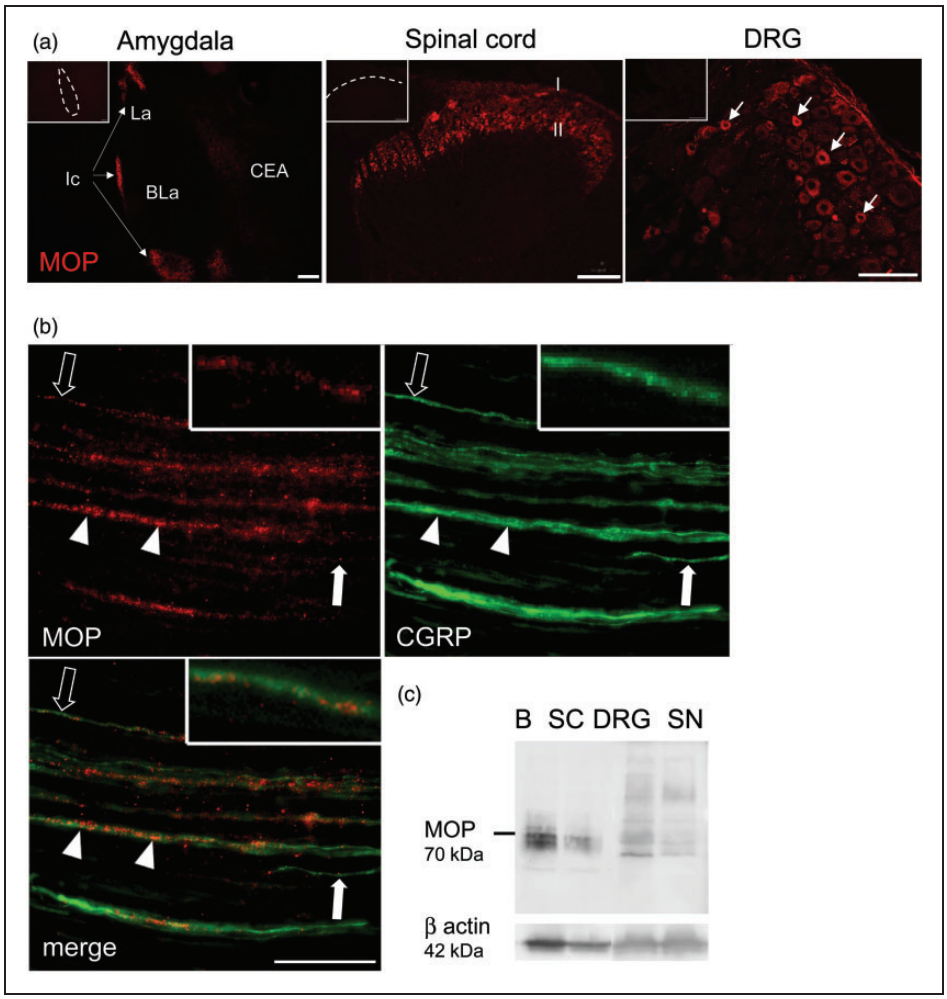

Figure 2. MOP-immunolabeling using a monoclonal antibody. Cryosections of amygdala, spinal cord, DRG, and sciatic nerve were incubated with RabMAb-MOP. MOP immunoreactivity was prominent in (a) the Ic of the amygdala (arrows, left panel), in superficial laminae I/II of spinal dorsal horn (middle panel) and in small/medium DRG neurons (arrows in right panel). Scale bars 100 μm. Controls (omission of the primary Ab) are displayed in the upper left corner (nuclei of the amygdala: CEA: central nucleus; La: lateral nucleus; BLa: basolateral nucleus). (b) Longitudinal sciatic nerve sections were stained with RabMAb-MOP (red) and the sensory fiber marker CGRP (green). Arrowheads and open arrows point to fibers/fiber bundles with comparatively high and low MOP immunoreactivity, respectively. Closed arrows point to fibers containing only CGRP (scale bar 20 μm). (c) Tissue lysates from rat brain (B), spinal cord (SC), DRG, and sciatic nerve (SN) were separated by electrophoresis, blotted, and reacted using RabMAb-MOP (70 kDa) and β-actin (42 kDa) (all representative images, $n = 3$).
MOP: μ-opioid receptor; DRG: dorsal root ganglion; CGRP: calcitonin gene-related peptide; Ic: intercalated nuclei.

amygdala, in lamina I and II of the dorsal horn in the spinal cord and in small/medium-sized neurons of DRG (Figure 3(a)) in MOP-mcherry knock-in mice. Double labeling of knock-in mouse sciatic nerve preparations with anti-mcherry and anti-CGRP confirmed the presence of MOP-mcherry exclusively in CGRP fibers and fiber bundles (Figure 3(b)). MOP-mcherry immunofluorescence appeared more evenly distributed and less granular than MOP-immunofluorescence in the rat samples (see above). This was mainly due to a higher detection sensitivity of the system, since after UV-light-induced bleaching, intraaxonal fluorescent granules became detectable. Immunolabeling on WT mouse tissue was devoid of fluorescence in all analyzed tissues (data not shown). In Western blot, we detected MOP-mcherry (predicted size 80 kDa) in brain, spinal cord, DRG, and sciatic nerve samples (Figure 3(c)), albeit with less protein and smaller and larger bands in the peripheral nervous tissue.[38]

Immunoelectron microscopic analyses indicate membrane localization of MOP in nociceptive axons

According to the results of the immunofluorescence experiments, detection of MOP using RabMAb-MOP in rat and of mcherry in MOP-mcherry knock-in mice

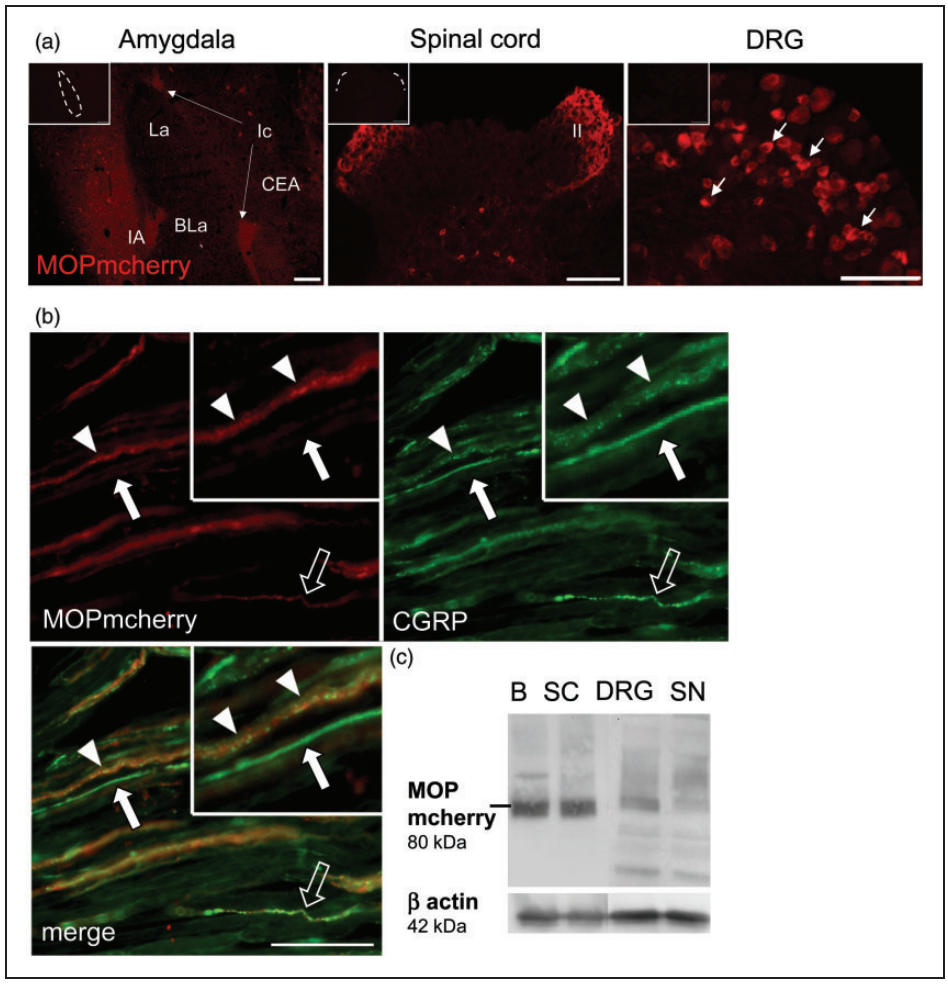

Figure 3. MOP-mcherry immunodetection in knock-in mice. (a) Immunolabeling in cryosections is shown in amygdala (left panel), superficial laminae I/II of spinal dorsal horn (middle panel), and small/medium DRG neurons (right panel). Controls testing for unspecific antibody binding are inserted in the upper left corner (scale bars 100 μm, nuclei of the amygdala: CEA: central nucleus; La: lateral nucleus; BLa: basolateral nucleus; Ic: intercalated nuclei). (b) Longitudinal section of MOP-mcherry knock-in sciatic nerve labeled for colocalization of MOP-mcherry (red) with CGRP (green) in putative nociceptive fibers and fiber bundles (arrowheads: high MOP-mcherry immunoreactivity; open arrow: low MOP-mcherry immunoreactivity; closed arrows: CGRP-ir only, scale bar 20 μm). (c) Western blots on tissues from MOP-mcherry mice confirm MOP-mcherry (80 kDa) localization in brain (B), spinal cord (SC), DRG, and sciatic nerve (SN) relative to β-actin (42 kDa) (all representative images, $n = 3$).
MOP: μ-opioid receptor; DRG: dorsal root ganglion; CGRP: calcitonin gene-related peptide.

provides the high detection specificity, sensitivity, and reproducibility required for reliable immunoelectron microscopic analyses of subcellular receptor distribution. Therefore, preembedding immunogold labeling was carried out on rat sciatic nerve using RabMAb-MOP (not shown) and on MOP-mcherry knock-in mouse sciatic nerve using mcherry antibody (Figure 4(a)). Ultrastructural analysis showed discrete silver-enhanced immunogold dots (IG) localized on Remak bundles containing tightly clustered axonal profiles surrounded by thin Schwann cell processes. Close inspection documented MOP/MOP-mcherry localization in the cytoplasm as well as at the membrane of unmyelinated axons. Silver-gold-dots were also occasionally seen on presumably non-nociceptive large myelinated axons, Schwann cell cytoplasm, and endoneurial tissue, as well as in control preparations (see below), indicating some unspecific labeling. Unspecific binding appeared overall higher in the RabMAb-MOP-reacted rat nerve sections than in the mouse preparation (not shown). Therefore, we decided to validate the ultrastructural localization analyses by diligent comparative analysis of preparations treated with/without mcherry antibody of MOP-mcherry knock-in and WT mouse sciatic nerve (MOP-mcherry-pos, MOP-mcherry-neg; WT-pos, WT-neg). In the MOP-mcherry-pos

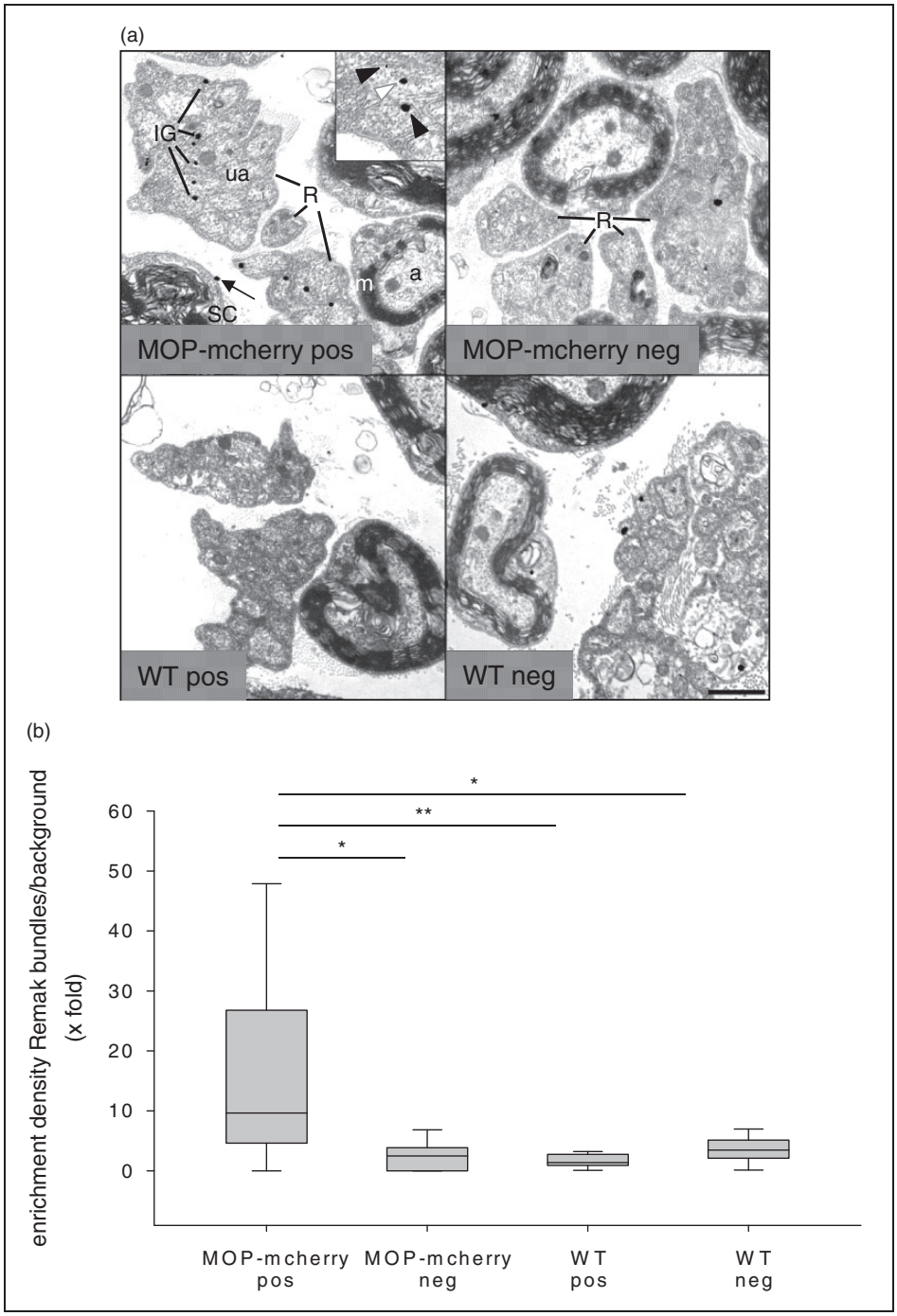

Figure 4. Ultrastructural immunolocalization of MOP-mcherry fusion protein in unmyelinated axons. (a) Ultrathin sections from sciatic nerve of MOP-mcherry knock-in (upper panel) and WT (lower panel) mouse incubated with mcherry antibody (MOP-mcherry-pos, WT-pos) or without primary antibody (MOP-mcherry-neg, WT-neg) and embedded in Epon. Black and white arrowheads in the inset point to silver-enhanced immunogold dots (IG) localized at the plasma membrane and in the cytoplasm of unmyelinated axons (ua) of Remak bundles (R), respectively, in the MOP-mcherry-pos preparation. IG on Remak bundles and myelinated fibers in the controls (WT-pos, MOP-mcherry-neg, WT-neg) represent unspecific labeling. The arrow in MOP-mcherry-pos points to presumably unspecific label in a Schwann cell (SC) (a: axon; m: myelin sheath). Scale bar 1 μm. (b) Quantification of immunogold dot distribution comparing the four experimental conditions is displayed as median (plus 25/75 percentile) dot density enrichment in Remak bundles over background ($\times$-fold) ($n = 10$–15; one-way ANOVA and post hoc Dunn's test on ranks; $^{*}p < 0.05$, $^{**}p < 0.01$).
MOP: μ-opioid receptor; WT: wild-type; ANOVA: analysis of variance.

preparation, the dot density over Remak bundles was significantly higher than background with median labeling enrichment (dot density over Remak bundles divided by dot density over myelinated fibers) of 10.6-fold (Figure 4(b)). MOP-mcherry immunoreactivity in small, thinly myelinated nociceptive Aδ-fibers was not specifically assessed since these fibers could not be unequivocally identified in the preparations. Thus, although background was determined mainly over large thickly myelinated fibers, labeling enrichment over Remak bundles may have even been underestimated due to inclusion of some specific labeling in the background counts.

To avoid bias due to differential unspecific binding properties of various tissue components, dot density in Remak bundles over background was determined also in the controls (MOP-mcherry-neg, WT-pos, WT-neg). The results here indeed indicated a higher dot density in Remak bundles compared to myelinated fibers (possibly caused by lower unspecific binding affinity of myelin). However, the medians of labeling enrichment in Remak bundles were only between 2.1- and 3.2-fold and were significantly lower than in MOP-mcherry-pos for all controls (Figure 4(b)). This suggests that the localization of the majority of a significant proportion of gold dots in unmyelinated axons (membrane and cytoplasm) in the MOP-mcherry-pos preparation specifically represents the subcellular localization of the fusion protein. Thus, the ultrastructural analysis indicates a membrane localization of MOP in unmyelinated (presumably nociceptive) axons of intact sciatic nerve.

Fentanyl and DAMGO inhibit depolarization-induced CGRP release from rat nerve axons

Isolated preparations of desheathed sciatic nerves can be stimulated to release CGRP by depolarization with potassium chloride.[30] To further assess functionality of axonal MOP, we tested whether opioids could inhibit CGRP release ex vivo. Treatment of desheathed nerves with both the hydrophilic opioid DAMGO (10 μM) and the lipophilic opioid fentanyl (1 μM) inhibited CGRP release stimulated by 60 mM potassium chloride (Figure 5(a) and (b)). Neither opioid alone had any effect on baseline CGRP release. DAMGO- or fentanyl-mediated inhibition of KCl-induced CGRP release was essentially absent if the MOP antagonist naloxone was added in equimolar concentrations (Figure 5(c) and (d)).

Further studies with fentanyl at different concentrations demonstrated that at least 100 nM are required for a significant inhibition of CGRP release stimulated by potassium chloride-evoked depolarization and EC_{50} was estimated to 630 nM (Figure 5(e)). Therefore, we conclude that functional MOPs are expressed in the axons of peptidergic primary afferent neurons.

Functionality of axonal MOP in vivo: Behavioral analysis after perisciatic fentanyl application

We have previously shown that hydrophilic opioid DAMGO (30 μg) does not increase mechanical nociceptive thresholds unless it is injected together with hypertonic saline (Figure 6(a)).[17] As demonstrated before, opioid-induced increases in mechanical nociceptive thresholds were specifically mediated by opioid receptors because the effect was completely reversed by coinjection of the MOP antagonist naloxone at concentrations as low as 0.1 ng (Figure 6(b)).[17] The antinociception-enhancing effect of hypertonic saline is presumably at least partly dependent on the opening of the perineurial barrier to allow for the access of DAMGO. However, since further effects of hypertonicity on the axons cannot be excluded, we wanted to assess whether axonal MOPs, which according to our ultrastructural study may be constitutively localized in nociceptive axonal membranes, are functional under completely physiological conditions. Therefore, we here asked whether perisciatic injection of the lipophilic opioid fentanyl, which can pass freely through the perineurial barrier, induces antinociception by itself. Application of 0.1 μg fentanyl significantly increased paw pressure thresholds (Figure 6(c)). A lower dose of fentanyl (0.01 μg) had no impact on mechanical nociceptive thresholds unless it was coinjected with hypertonic saline, indicating an additional effect of hypertonic saline on axonal MOP availability and functionality independent of barrier opening. Opioid-induced increases in nociceptive thresholds were completely reversed by simultaneous application of the MOP antagonist naloxone (Figure 6(d)). No change in paw pressure thresholds was seen in the contralateral paw indicating no systemic effect. Collectively, these data reveal that MOP is present and functional in completely intact nociceptive axons. Hypertonic saline treatment further enhances the function of axonal MOP in vivo.

Hypertonicity decreases MOP agonist-induced receptor internalization

Sucrose can block enkephalin- or etorphine-induced MOP internalization.[24] Thus, we hypothesized that hypertonic saline-induced enhancement of opioid action in vivo could be mediated by decreased internalization of receptors. To this end, we used a cellular system to visualize β-arrestin-2 recruitment using human embryonic kidney (HEK)-293 cells transfected with β-arrestin-2-yellow fluorescent protein (YFP) and human MOP-cyan fluorescent protein (CFP).

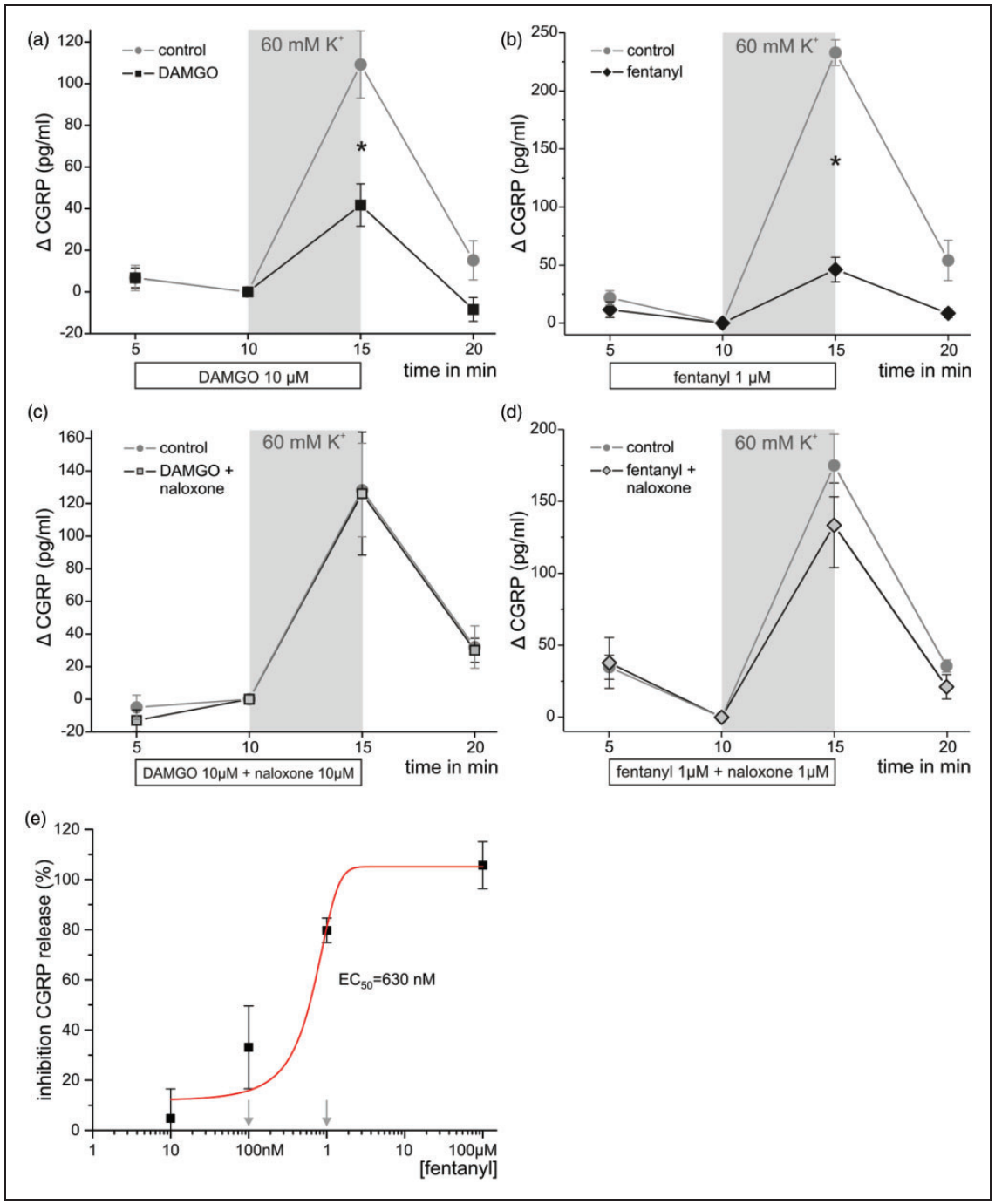

Figure 5. Opioids inhibit potassium-induced CGRP release from rat sciatic nerves via MOP. Desheathed sciatic nerves isolated from rats were preincubated with DAMGO (10 µM, a, $n = 8$), fentanyl (1 µM, b, $n = 4$), and each together with the opioid receptor antagonist naloxone (10 µM, c, and 1 µM, d, respectively) for 5 min. In the presence of the opioids, CGRP release was induced with 60 mM KCl (shed gray area). (e) Percent inhibition of KCl-responses was tested at different concentrations of fentanyl (10 nM–100 µM, $n = 4$–8) and the corresponding EC_{50} was calculated by fitting to the Boltzmann equation. Naloxone was tested at equimolar concentrations against fentanyl 0.1 and 1 µM, which is indicated by downward arrows (*$p < 0.05$ calculated by one-way ANOVA with Scheffé post hoc test). Data are presented as means ± SEM.

MOP: µ-opioid receptor; DAMGO: [D-Ala^2, N-MePhe^4, Gly-ol]-enkephalin; CGRP: calcitonin gene-related peptide; ANOVA: analysis of variance.

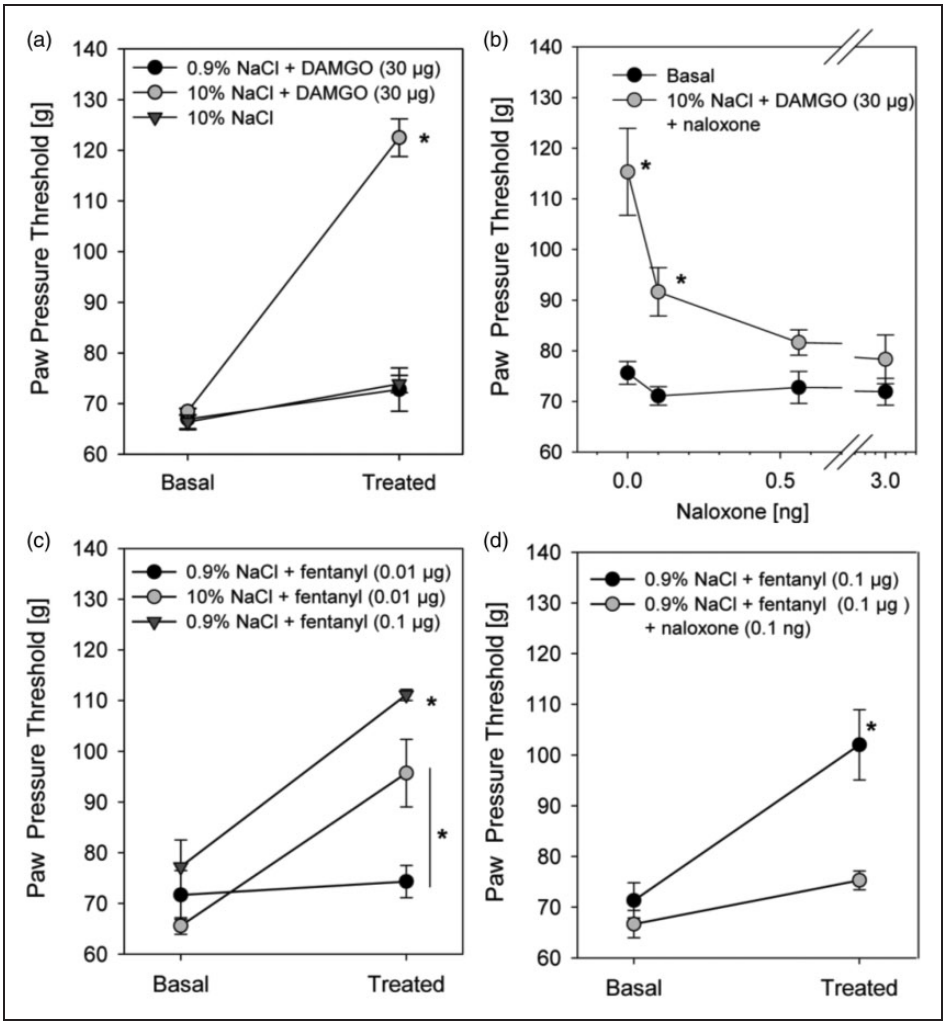

Figure 6. Perineurial application of the MOP agonists, DAMGO and fentanyl, increase mechanical nociceptive thresholds-improved function in the presence of hypertonic saline. Wistar rats were injected at the sciatic nerve with DAMGO (30 µg, a) or fentanyl in two different doses (0.01 or 0.1 µg, c) together with hypertonic (10% NaCl) or normal saline (0.9% NaCl). (b, d) In selected experiments, DAMGO and fentanyl were applied together with the opioid receptor antagonist naloxone. In all experiments, paw pressure thresholds were measured right before ("basal") and 10 min ("treated") after application of DAMGO or fentanyl (all $n = 6$, two-way ANOVA, Bonferroni post hoc correction, $^*p < 0.05$). Data are presented as means ± SEM.
MOP: µ-opioid receptor; DAMGO: [D-Ala^2, N-MePhe^4, Gly-ol]-enkephalin; ANOVA: analysis of variance.

Treatment with DAMGO reduced the intensity of the β-arrestin-2 signal in the cytosol by 35% within 120 s consistent with a recruitment of β-arrestin-2 to the membrane after MOP activation. This initial receptor/β-arrestin-2 interaction initialized internalization of DAMGO-MOP and over time the complex dissociated. Cytosolic β-arrestin-2 increased again and a punctuate pattern of internalized MOP-CFP could be seen (Figure 7(a) and (d)). Pretreatment with 200 mM NaCl for 5 min did not influence initial β-arrestin-2 recruitment to the membrane but prevented the subsequent increase in the cytosolic β-arrestin-2 signal, indicating an inhibition of the internalization of the DAMGO-MOP – β-arrestin-2 complex by hypertonicity (Figure 7(b) and (d)). To verify the involvement of dynamin as a complex to regulate clathrin-induced internalization of MOP, cells were treated with dynasore.[39] This treatment again had no effect on β-arrestin recruitment to the membrane but also prevented internalization of the DAMGO-MOP – β-arrestin complex (Figure 7(c) and (d)).

Next, we also evaluated the effect of fentanyl on β-arrestin-2 recruitment and internalization. Similar to DAMGO, fentanyl application reduced the intensity of the β-arrestin-2 signal in the cytosol by 30% compatible with rapid β-arrestin-2 recruitment (Figure 7(e) and (h)). Subsequently, the signal reappeared consistent with an internalization of the MOP as seen by the punctuate

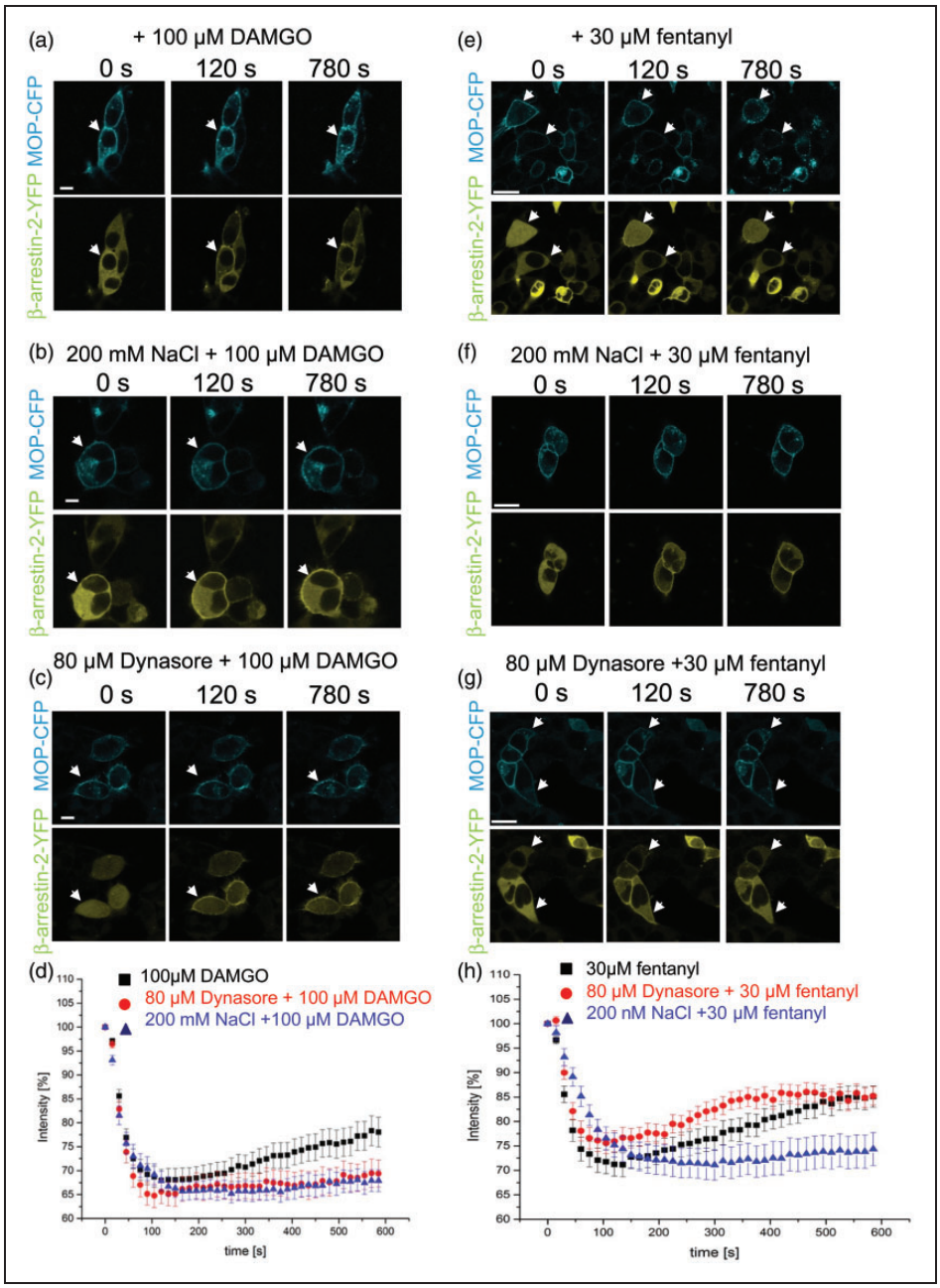

Figure 7. MOP agonist-mediated β-arrestin-2 recruitment: Inhibition of cytosolic β-arrestin-2 reappearance and thereby MOP internalization by hypertonic saline. (a to c, e to g) Images from HEK-293 triple transfected with MOP-CFP (*cyan*, upper row), GRK2, and β-arrestin-2-YFP (*yellow*, lower row) are shown at 0, 120, or 780 s after application of 100 μM DAMGO (a to c) or 30 μM fentanyl (e–g). Cells were preincubated with 200 mM NaCl for 5 min (b, f) or with 80 µM dynasore for 30 min (c, g) followed by application of DAMGO or fentanyl (representative examples; arrows: membrane β-arrestin-2; scale bars = 10 µm). (d, h) Images were quantified and corrected for photobleaching as described under "Material and Methods" *Black squares* (DAMGO or fentanyl), *red circles* (preincubation with dynasore followed by DAMGO or fentanyl), *blue triangles* (preincubation with 200 mM NaCl followed by DAMGO or fentanyl) (DAMGO: $n = 42$ cells, 22 cells, or 25 cells, respectively; fentanyl: $n = 31$ cells, 22 cells, or 20 cells, respectively, all six to nine different experiments, at least three different transfections).

DAMGO: [D-Ala^2, N-MePhe^4, Gly-ol]-enkephalin; YFP: yellow fluorescent protein; MOP-CFP: µ-opioid receptor-cyan fluorescent protein; HEK: human embryonic kidney; GRK2: G protein-coupled receptor kinase 2.

pattern of internalized MOP-CFP, which was inhibited if cells were pretreated with hypertonic saline (Figure 7(f) and (h)). Dynasore did not inhibit internalization of fentanyl-MOP – β-arrestin complex (Figure 7(g) and (h)), while β-arrestin-2 started to accumulate again in the cytosol.

In summary, hypertonic environment attenuates fentanyl- or DAMGO-induced MOP – β-arrestin-2 internalization in an in vitro system.

Discussion

In the present study, we demonstrate by light and electron microscopic analyses that opioid receptors are present at plasma membranes of peripheral sensory axons. Application of lipophilic opioids at the sciatic nerve increased mechanical nociceptive thresholds and inhibited CGRP release. Treatment with hypertonic saline further enhances fentanyl-induced increases in nociceptive thresholds. In recombinant cellular systems, opioids induced β-arrestin-2 recruitment and subsequent MOP internalization. This was prevented by hypertonic stress. This mechanism could increase the availability of MOP on the cell surface within seconds as a possible mechanism of enhanced opioid receptor function due to treatment with hypertonic saline in vivo.

Detection of peripheral axonal opioid receptors

Antibodies against MOP[40] and also DOP[40,41] have long been discussed regarding their specificity in Western blots and immunohistochemistry. For example, Schmidt et al.[3] observed specific staining in the brain and spinal cord but not in the DRG using MOP-knockout mice as controls. Additionally, MOP immunoreactivity is comparatively low in intact sciatic nerve[3,42] so that particularly high signal-to-noise ratio of the detection is required to enable reliable and reproducible identification. Here, we yielded specific but low-intensity MOP immunoreactivity in the undamaged rat sciatic nerve using RabMAb-MOP. Importantly, immunoreactions lacked significant labeling outside CGRP-positive fibers and fiber bundles. Interestingly, the relative immunolabeling intensity for MOP and CGRP differed between individual axons and in axon bundles, indicating presence of MOP at varying levels in different sensory (e.g. nociceptive) axon types in naïve rats. Additionally, we verified our findings in a knock-in mouse line expressing MOP fused to the red fluorescent mcherry protein.[25] Our results confirm differential MOP-localization solely in CGRP-ir sensory fibers and fiber bundles of the sciatic nerve also in mice.

Specificity of antibody staining is a necessary prerequisite for successful detection of subcellular protein localization using immunoelectron microscopy. The similarity in light microscopic immunolabeling patterns documented in the present study for MOP in rat and mcherry in the knock-in mouse sciatic nerve sciatic nerve validates that localization of the MOP-mcherry fusion protein represents the localization of MOP in the sciatic nerve also in non-genetically modified animals. Diligent analyses including several controls suggested that preembedding mcherry-immunolabeling in mcherry knock-in mouse sciatic nerve represents cell-specific subcellular localization of the fusion protein, and thus of MOP in rodent sciatic nerve. Taken together, the results indicate that MOP is constitutively present not only at the nerve terminals but also along the membranes of non-myelinated, presumably nociceptive axons of sciatic nerves. RabMAb-MOP stainings in rat sciatic nerves provide lower signal-to-noise ratio, similar to what was observed in the light microscopical preparations. However, further methodological improvements might enable quantitative analysis also of immunoelectron microscopic results using direct MOP labeling.

Functional opioid receptors in axons: Inhibition of CGRP release and increases in nociceptive thresholds

Binding of opioids to MOP reduces nociceptive signal transmission at central Aδ- and C-fiber synapses by inhibition of presynaptic N-type voltage-dependent Ca^{2+} channels. P/Q-type voltage-dependent Ca^{2+} channels and the Ca^{2+}-dependent transmitter release machinery are also targets of opioids[43] especially in the peripheral nervous system.[22] Here, both fentanyl and DAMGO prevented depolarization-induced CGRP release from the sciatic nerve in vitro. These results differ from other studies,[44] because morphine and deltorphin as a DOP agonist alone could not inhibit depolarization-induced CGRP release from desheathed nerves. Only the sequential administration of deltorphin and morphine blocked CGRP release. DAMGO (100 nM) slightly, but not significantly, inhibited KCl-induced CGRP release. The contrast to our work may be explained, because substantially lower concentrations of both MOP agonists were applied and non-desheathed nerves were used, which prevents penetration of peptides like DAMGO and CGRP and hinders permeation of hydrophilic opioids through the intact epi-perineurium.

Evidence of axonal function of opioid receptors was shown in mice with neuropathic pain after sciatic nerve ligation.[3,9–11] However, the function of opioid receptors in the absence of neuropathy remains controversial. Here, we provide evidence that axonal opioid receptors are functional and increase nociceptive thresholds even in undamaged nerves, if lipophilic opioids are used. Opioid-induced antinociception was not an unspecific local anesthetic-like effect,[45] because it was fully blocked by naloxone as seen before.[17] Treatment with hypertonic saline further enhanced opioid-mediated antinociception

as indicated by lower dose of fentanyl necessary to elicit an effect.

In summary, MOP activation ex vivo reduces stimulated CGRP release from peripheral axons and can increase nociceptive thresholds, indicating that opioid receptors, like other receptors important for nociceptive signal transduction, are not solely transported along the axon but can also be effectively inserted into the axolemma to become functionally competent and couple to signaling pathways suited to inhibit nociceptor function.

Hypertonic solution: Opioid function in vivo and MOP internalization in vitro

The behavioral studies indicate that hypertonic saline treatment induces increased availability and/or functionality of MOP in peripheral sensory axons. This could be due to transient local increase of MOP insertion and presence in axonal membranes caused possibly via a local block of axonal transport. An augmented membrane insertion of axonal MOP might lead to extended opioid effects possibly via decreased receptor desensitization. Hypertonic solutions (high concentrations of sucrose) inhibit internalization of receptors,[24,46] but no studies have been done using hypertonic saline and MOP. Fentanyl and DAMGO – in contrast to morphine – both induce internalization of MOP via a dynamin-mediated process. Dynasore is a small molecule GTPase inhibitor that targets dynamin-1, dynamin-2, and dynamin-related protein 1 (Drp1). It blocks dynamin-dependent endocytosis, because it inhibits the scission of endocytic vesicles. Here, we used dynasore as a positive control to prevent dynamin-mediated internalization of MOP after DAMGO activation.

In transfected cells, fentanyl as well as DAMGO rapidly promoted β-arrestin-2 recruitment to the membrane and subsequent internalization of the complex. Redistribution of β-arrestin-2 to the cytosol and thereby internalization was impeded by hypertonic saline. Dynasore blocked internalization of DAMGO but not of fentanyl. An explanation could be a less tight complex formation between fentanyl-MOP/β-arrestin-2 compared to DAMGO-MOP/β-arrestin-2. DAMGO mediates MOP phosphorylation at the key residue serine-375 via G protein-coupled receptor kinase 2 (GRK2) and GRK3,[47] while fentanyl mediates MOP phosphorylation at this site via GRK3.[48] This residue needs to be phosphorylated prior to further phosphorylation on other sites of the MOP (for a recent review on the complex issue of MOP phosphorylation, we refer to Allouche et al.[49]). Since we only used GRK2 for cotransfection, the endogenous kinase expression of GRK3 in our HEK cells might be limiting in the case of fentanyl, which might lead to less complete phosphorylation pattern of the receptor. Given that the number of phosphates has been shown to be important for receptor/arrestin complex affinity,[50] this could be an explanation for this observation.

The differences observed between treatment with dynasore and hypertonic solution have to be discussed in the light of the fact that sodium ions can act as allosteric enhancers of ligand affinity at G protein-coupled receptors (GPCRs) including DOP,[51,52] and we used 200 mM sodium chloride solution as the hypertonic stimulus. Indeed, recent data point toward sodium's role as a potential cofactor in class A GPCR function.

Nonetheless, hypertonic saline inhibits internalization of agonist-MOP complexes, which could also be a mechanism why MOP function is increased after treatment with hypertonic saline. The process remains to be completely elucidated. Hypertonic treatment causes coated pits to disappear and induces abnormal clathrin polymerization.[53,54] In conclusion, hypertonic saline prevents receptor internalization or might change the ligand affinity ultimately leading to improved receptor function.

Conclusion

MOPs are functionally expressed along the membrane of the peripheral nerve axons and can be targeted by opioids to inhibit nociception in vivo in naive rats and CGRP release in vitro. Hypertonic saline may increase MOP membrane availability, which could account for enhanced MOP function. The immunolabeling protocols using specific MOP detection methods developed in the present study will aid future analyses on peripheral axonal MOP localization and function.

Opioids can be effective in regional anesthesia in patients as long as they can penetrate the perineurial barrier. However, it is worthwhile to further explore various methods of increasing functionality of MOP in axons to improve selective targeting of nociceptive neurons inducing analgesia without impairing motor or sensory function.

Acknowledgments

We are indebted to K Reinfurth-Gehm and K Langenbrink for competent technical assistance and to Dr Dagmar Hackel contributing pain behavior experiments.

Author Contributions

EMM carried out the immunohistochemical, ultrastructure studies, and Western blot and drafted the manuscript. KK performed and analyzed the CGRP release experiments, SM the transfection and live cell imaging. DM and BLK created the MOP-mcherry mice and helped with genotyping and breeding. CH and PWR participated in the design of the study and performed the data analysis of life cell imaging and CGRP release, respectively. HLR, AB as well as EA conceived the study, designed the experiments, and wrote the manuscript. All authors read and approved the final manuscript. EA and HLR contributed equally to this work.

Declaration of Conflicting Interests

The author(s) declared the following potential conflicts of interest with respect to the research, authorship, and/or publication of this article: The authors declare that they have no competing interests.

Funding

The author(s) disclosed receipt of the following financial support for the research, authorship, and/or publication of this article: This study was supported by the IZKF (to EMM, EA, HLR, and AB) and funds of the Department of Anesthesiology, University Hospital of Wuerzburg (to HLR and AB), as well as by the Wilhelm Sander-Stiftung (to KK and PWR). The publication was funded by the German Research Foundation (DFG) and the University of Wuerzburg in the funding program Open Access Publishing.

References

1. Stein C, Schäfer M and Machelska H. Attacking pain at its source; new perspectives on opioids. *Nat Med* 2003; 9: 1003–1008.
2. Lee LA, Caplan RA, Stephens LS, et al. Postoperative opioid-induced respiratory depression: a closed claims analysis. *Anesthesiology* 2015; 122: 659–665.
3. Schmidt Y, Gaveriaux-Ruff C and Machelska H. Mu-opioid receptor antibody reveals tissue-dependent specific staining and increased neuronal mu-receptor immunoreactivity at the injured nerve trunk in mice. *PLoS One* 2013; 8: e79099.
4. Hassan AH, Ableitner A, Stein C, et al. Inflammation of the rat paw enhances axonal transport of opioid receptors in the sciatic nerve and increases their density in the inflamed tissue. *Neuroscience* 1993; 55: 185–195.
5. Coggeshall RE, Zhou S and Carlton SM. Opioid receptors on peripheral sensory axons. *Brain Res* 1997; 764: 126–132.
6. Brack A, Rittner HL, Machelska H, et al. Endogenous peripheral antinociception in early inflammation is not limited by the number of opioid-containing leukocytes but by opioid receptor expression. *Pain* 2004; 108: 67–75.
7. Rittner HL, Hackel D, Voigt P, et al. Mycobacteria attenuate nociceptive responses by formyl peptide receptor triggered opioid peptide release from neutrophils. *PLoS Pathogens* 2009; 5: e1000362.
8. Rittner HL, Hackel D, Yamdeu RS, et al. Antinociception by neutrophil-derived opioid peptides in noninflamed tissue – role of hypertonicity and the perineurium. *Brain Behav Immun* 2009; 23: 548–557.
9. Labuz D and Machelska H. Stronger antinociceptive efficacy of opioids at the injured nerve trunk than at its peripheral terminals in neuropathic pain. *J Pharmacol Exp Ther* 2013; 346: 535–544.
10. Labuz D, Schmidt Y, Schreiter A, et al. Immune cell-derived opioids protect against neuropathic pain in mice. *J Clin Invest* 2009; 119: 278–286.
11. Truong W, Cheng C, Xu QG, et al. Mu opioid receptors and analgesia at the site of a peripheral nerve injury. *Ann Neurol* 2003; 53: 366–375.
12. Tsai YC, Won SJ and Lin MT. Effects of morphine on immune response in rats with sciatic constriction injury. *Pain* 2000; 88: 155–160.
13. Grant GJ, Vermeulen K, Zakowski MI, et al. Perineural antinociceptive effect of opioids in a rat model. *Acta Anaesthesiol Scand* 2001; 45: 906–910.
14. Picard PR, Tramer MR, McQuay HJ, et al. Analgesic efficacy of peripheral opioids (all except intra-articular): a qualitative systematic review of randomised controlled trials. *Pain* 1997; 72: 309–318.
15. Flamer D and Peng PW. Intravenous regional anesthesia: a review of common local anesthetic options and the use of opioids and muscle relaxants as adjuncts. *Local Reg Anesth* 2011; 4: 57–76.
16. Dabrowski S, Staat C, Zwanziger D, et al. Redox-sensitive structure and function of the first extracellular loop of the cell-cell contact protein claudin-1: lessons from molecular structure to animals. *Antioxid Redox Signal* 2015; 22: 1–14.
17. Hackel D, Krug SM, Sauer RS, et al. Transient opening of the perineurial barrier for analgesic drug delivery. *Proc Natl Acad Sci U S A* 2012; 109: E2018–E2027.
18. Sauer RS, Krug SM, Hackel D, et al. Safety, efficacy, and molecular mechanism of claudin-1-specific peptides to enhance blood-nerve-barrier permeability. *J Control Release* 2014; 185: 88–98.
19. Antonijevic I, Mousa SA, Schäfer M, et al. Perineurial defect and peripheral opioid analgesia in inflammation. *J Neurosci* 1995; 15: 165–172.
20. Williams JT, Ingram SL, Henderson G, et al. Regulation of mu-opioid receptors: desensitization, phosphorylation, internalization, and tolerance. *Pharmacol Rev* 2013; 65: 223–254.
21. Nockemann D, Rouault M, Labuz D, et al. The K(+) channel GIRK2 is both necessary and sufficient for peripheral opioid-mediated analgesia. *EMBO Mol Med* 2013; 5: 1263–1277.
22. Baillie LD, Schmidhammer H and Mulligan SJ. Peripheral mu-opioid receptor mediated inhibition of calcium signaling and action potential-evoked calcium fluorescent transients in primary afferent CGRP nociceptive terminals. *Neuropharmacology* 2015; 93: 267–273.
23. Frölich N, Dees C, Paetz C, et al. Distinct pharmacological properties of morphine metabolites at G(i)-protein and beta-arrestin signaling pathways activated by the human mu-opioid receptor. *Biochem Pharmacol* 2011; 81: 1248–1254.
24. Keith DE, Murray SR, Zaki PA, et al. Morphine activates opioid receptors without causing their rapid internalization. *J Biol Chem* 1996; 271: 19021–19024.
25. Erbs E, Faget L, Scherrer G, et al. A mu-delta opioid receptor brain atlas reveals neuronal co-occurrence in subcortical networks. *Brain Struct Funct* 2015; 220: 677–702.
26. Zimmermann M. Ethical guidelines for investigations of experimental pain in conscious animals. *Pain* 1983; 16: 109–110.
27. Bonn M, Schmitt A, Lesch KP, et al. Serotonergic innervation and serotonin receptor expression of NPY-producing neurons in the rat lateral and basolateral amygdaloid nuclei. *Brain Struct Funct* 2013; 218: 421–435.

28. Reynolds ES. The use of lead citrate at high pH as an electron-opaque stain in electron microscopy. *J Cell Biol* 1963; 17: 208–212.
29. Mousa SA, Zhang Q, Sitte N, et al. Beta-endorphin-containing memory-cells and mu-opioid receptors undergo transport to peripheral inflamed tissue. *J Neuroimmunol* 2001; 115: 71–78.
30. Sauer SK, Bove GM, Averbeck B, et al. Rat peripheral nerve components release calcitonin gene-related peptide and prostaglandin E2 in response to noxious stimuli: evidence that nervi nervorum are nociceptors. *Neuroscience* 1999; 92: 319–325.
31. Bretag AH. Synthetic interstitial fluid for isolated mammalian tissue. *Life Sci* 1969; 8: 319–329.
32. Puehler W, Zöllner C, Brack A, et al. Rapid upregulation of mu opioid receptor mRNA in dorsal root ganglia in response to peripheral inflammation depends on neuronal conduction. *Neuroscience* 2004; 129: 473–479.
33. Schäfer M, Zhou L and Stein C. Cholecystokinin inhibits peripheral opioid analgesia in inflamed tissue. *Neuroscience* 1998; 82: 603–611.
34. Rittner HL, Mousa SA, Labuz D, et al. Selective local PMN recruitment by CXCL1 or CXCL2/3 injection does not cause inflammatory pain. *J Leukoc Biol* 2006; 79: 1022–1032.
35. Krasel C, Bunemann M, Lorenz K, et al. Beta-arrestin binding to the beta2-adrenergic receptor requires both receptor phosphorylation and receptor activation. *J Biol Chem* 2005; 280: 9528–9535.
36. Hoffmann C, Ziegler N, Reiner S, et al. Agonist-selective, receptor-specific interaction of human P2Y receptors with beta-arrestin-1 and -2. *J Biol Chem* 2008; 283: 30933–30941.
37. Pinard CR, Mascagni F and McDonald AJ. Medial prefrontal cortical innervation of the intercalated nuclear region of the amygdala. *Neuroscience* 2012; 205: 112–124.
38. Huang P, Chen C and Liu-Chen LY. Detection of mu opioid receptor (MOPR) and its glycosylation in rat and mouse brains by western blot with anti-muC, an affinity-purified polyclonal anti-MOPR antibody. *Methods Mol Biol* 2015; 1230: 141–154.
39. Patierno S, Anselmi L, Jaramillo I, et al. Morphine induces mu opioid receptor endocytosis in guinea pig enteric neurons following prolonged receptor activation. *Gastroenterology* 2011; 140: 618–626.
40. Niwa H, Rowbotham DJ and Lambert DG. Evaluation of primary opioid receptor antibodies for use in western blotting. *Br J Anaesth* 2012; 108: 530–532.
41. Scherrer G, Imamachi N, Cao YQ, et al. Dissociation of the opioid receptor mechanisms that control mechanical and heat pain. *Cell* 2009; 137: 1148–1159.
42. Khalefa BI, Shaqura M, Al-Khrasani M, et al. Relative contributions of peripheral versus supraspinal or spinal opioid receptors to the antinociception of systemic opioids. *Eur J Pain* 2012; 16: 690–705.
43. Heinke B, Gingl E and Sandkuhler J. Multiple targets of mu-opioid receptor-mediated presynaptic inhibition at primary afferent Adelta- and C-fibers. *J Neurosci* 2011; 31: 1313–1322.
44. Schramm CL and Honda CN. Co-administration of delta- and mu-opioid receptor agonists promotes peripheral opioid receptor function. *Pain* 2010; 151: 763–770.
45. Leffler A, Frank G, Kistner K, et al. Local anesthetic-like inhibition of voltage-gated Na(+) channels by the partial mu-opioid receptor agonist buprenorphine. *Anesthesiology* 2012; 116: 1335–1346.
46. Jarousse N and Kelly RB. Selective inhibition of adaptor complex-mediated vesiculation. *Traffic* 2000; 1: 378–384.
47. Doll C, Konietzko J, Poll F, et al. Agonist-selective patterns of micro-opioid receptor phosphorylation revealed by phosphosite-specific antibodies. *Br J Pharmacol* 2011; 164: 298–307.
48. Glück L, Loktev A, Mouledous L, et al. Loss of morphine reward and dependence in mice lacking G protein-coupled receptor kinase 5. *Biol Psychiatry* 2014; 76: 767–774.
49. Allouche S, Noble F and Marie N. Opioid receptor desensitization: mechanisms and its link to tolerance. *Front Pharmacol* 2014; 5: 280.
50. Vishnivetskiy SA, Gimenez LE, Francis DJ, et al. Few residues within an extensive binding interface drive receptor interaction and determine the specificity of arrestin proteins. *J Biol Chem* 2011; 286: 24288–24299.
51. Katritch V, Fenalti G, Abola EE, et al. Allosteric sodium in class A GPCR signaling. *Trends Biochem Sci* 2014; 39: 233–244.
52. Fenalti G, Giguere PM, Katritch V, et al. Molecular control of delta-opioid receptor signalling. *Nature* 2014; 506: 191–196.
53. Heuser JE and Anderson RG. Hypertonic media inhibit receptor-mediated endocytosis by blocking clathrin-coated pit formation. *J Cell Biol* 1989; 108: 389–400.
54. McMahon HT and Boucrot E. Molecular mechanism and physiological functions of clathrin-mediated endocytosis. *Nat Rev Mol Cell Biol* 2011; 12: 517–533.